


# Quantitative assessment of the oxygen isotope composition of fish otoliths from Lake Mungo, Australia

Kelsie Long<sup>a,b,c,\*</sup> , David Heslop<sup>a</sup>, Eelco J. Rohling<sup>a,d</sup>

<sup>a</sup>Research School of Earth Sciences, Australian National University, 142 Mills Road, Canberra, ACT 2601, Australia

<sup>b</sup>School of Culture, History and Language, Australian National University, H.C. Coombs building, 9 Fellows Road, Canberra, ACT 2601, Australia

<sup>c</sup>ARC Centre of Excellence for Australian Biodiversity and Heritage, Australian National University, Canberra, ACT 2601, Australia

<sup>d</sup>School of Ocean and Earth Science, University of Southampton, National Oceanography Centre, Southampton, SO15 3ZH, UK

\*Corresponding author e-mail address: [Kelsie.long@anu.edu.au](mailto:Kelsie.long@anu.edu.au).

(RECEIVED August 26, 2020; ACCEPTED December 1, 2020)

## Abstract

The Willandra Lakes region is a series of once interconnected and now-dry lake basins in the arid zone of southeastern Australia. It is a UNESCO World Heritage Site of cultural, archaeological, and geological significance, preserving records of Aboriginal occupation and environmental change stretching back to at least 50 ka. Linking the archaeology with the commensurate palaeoenvironmental information is complicated by the millennial time spans represented by the past hydrological record preserved in the sediment vs. the subdecadal evidence of each archaeological site. Oxygen isotope records across annual growth rings of fish otoliths (ear stones) can elucidate flooding and drying regimes on subannual scales. Otoliths from hearth sites (fireplaces) link lake hydrology with people eating fish on the lakeshore. Oxygen isotopic trends in hearth otoliths from the last glacial maximum (LGM) were previously interpreted in terms of high evaporation under dry conditions. However, this ignored hydrology-driven changes in water  $\delta^{18}\text{O}$ . Here, a mass balance model is constructed to test the effect lake desiccation has on water  $\delta^{18}\text{O}$  and how this compares with the LGM otolith records. Based on this modelling, we suggest that Lake Mungo otolith signatures are better explained by evaporation acting on full lakes rather than by lake drying.

**Keywords:** Quaternary; Oxygen isotopes; Willandra Lakes; Otoliths; Arid zone

## INTRODUCTION AND BACKGROUND

Lake Mungo is one of a series of now-dry lake basins that make up the Willandra Lakes UNESCO World Heritage Site in arid southeastern Australia (Fig. 1). It is one of the earliest archaeological sites in the country and has the oldest human cremation and ritual ochre burial in the world (Mungo I and III), dated to  $41 \pm 4$  ka (Bowler et al., 2003; Olley et al., 2006). A key feature of Lake Mungo is the lake-side sand and clay dunes (lunettes), which preserve a sedimentary record of alternating wet and dry conditions over the past 100 ka (Bowler, 1998; Bowler et al., 2012; Fitzsimmons et al., 2014; Jankowski et al., 2020). As these lunettes formed, they covered archaeological material, preserving a record of past life and environments. The relationship between periods of human occupation and

palaeoenvironmental changes has been a major research theme in the area, with initial studies predominantly concentrating on the stratigraphy and archaeology preserved at the southern tip of the Mungo lunette (Bowler et al., 1970; Bowler, 1998). More recent work, conducted as part of the ongoing Mungo Archaeology Project (MAP), has focused on the central lunette area, where widespread erosion has uncovered an array of stratigraphic units and archaeological features (Fitzsimmons et al., 2014; Stern, 2015; Barrows et al., 2020; Jankowski et al., 2020). Among these archaeological traces are thousands of fish otoliths that, when found in hearth sites (cooking fireplaces), provide an opportunity to link conditions in the lake directly with an Aboriginal presence on the lakeshore.

Otoliths grow in the inner ears of bony fish through the incremental deposition of calcium carbonate (aragonite) in periodic, usually annual, rings (Campana, 1999). The oxygen isotope ( $\delta^{18}\text{O}$ ) composition of fish otoliths is controlled by the temperature and  $\delta^{18}\text{O}$  of the water in which the fish lived. The  $\delta$  notation used here represents the ratio of  $^{18}\text{O}$  to  $^{16}\text{O}$  relative to that in a standard material, Vienna

**Cite this article:** Long, K., Heslop, D., Rohling, E. J. 2021. Quantitative assessment of the oxygen isotope composition of fish otoliths from Lake Mungo, Australia. *Quaternary Research* 102, 234–246. <https://doi.org/10.1017/qua.2020.121>

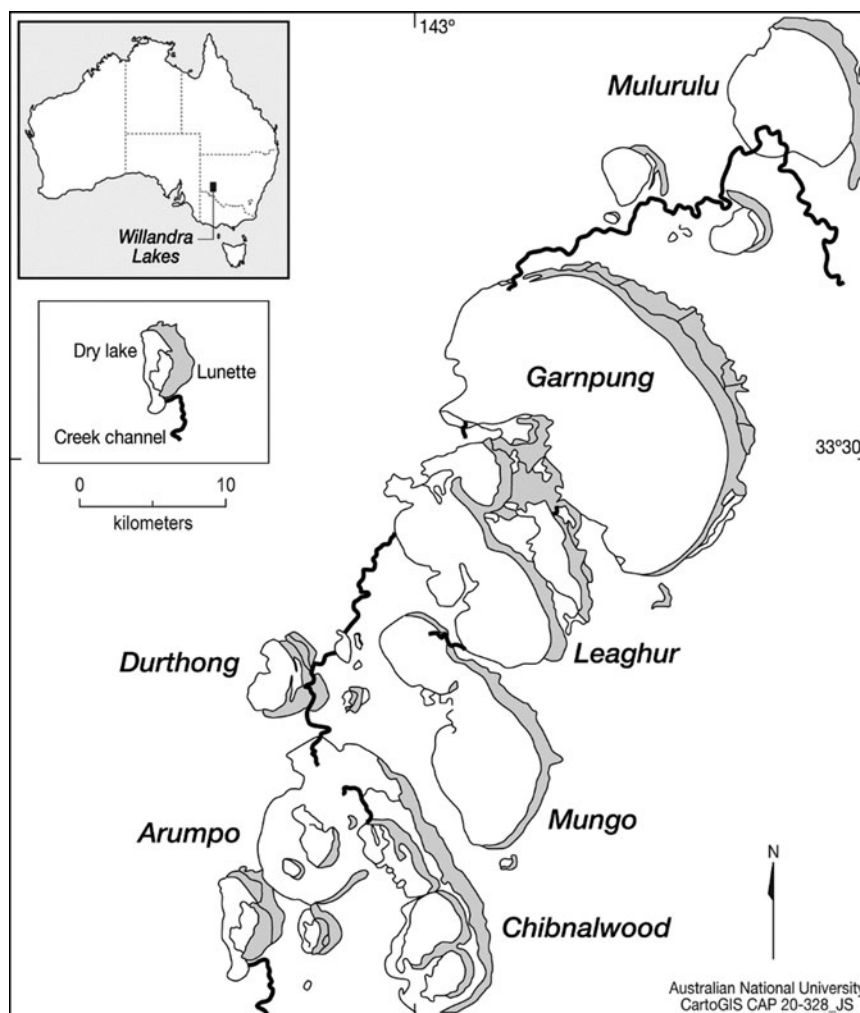


**Figure 1.** Map of the northern part of the Willandra Lakes system showing, among others, Mulurulu, Garnpung, Leaghur, and Mungo, which are the main lakes used in the model (adapted from Bowler 1998).

Pee Dee Belemnite for carbonates (otoliths) and Vienna Standard Mean Ocean Water for water. If the ambient water  $\delta^{18}\text{O}$  remains constant, a change of 1‰ in otolith  $\delta^{18}\text{O}$  values would reflect a  $\sim 4^\circ\text{C}$  change in water temperature (Kalish, 1991). In marine settings, where water oxygen isotopes are fairly stable over time, seasonal temperature changes can be detected in the otolith and other biogenic carbonate oxygen isotopes (Weidman and Millner, 2000; Andrus et al., 2002; Mannino et al., 2008; Geffen et al., 2011). At freshwater sites, the  $\delta^{18}\text{O}$  of ambient water is variable, changing with precipitation, flooding, and evaporation. These water composition changes tend to dominate the  $\delta^{18}\text{O}$  record of otoliths and other carbonate remains in these environments (Leng and Marshall, 2004; Leng and Lewis, 2014; Dufour et al., 2018; Long et al., 2018). Therefore, consideration of the hydrological controls inherent within the system as a whole is crucial for the correct interpretation of the geochemical traces preserved in otoliths.

Some have described the Willandra Lakes region as so lacking in surface water and so windy and dusty that it was uninhabited during the last glacial maximum (LGM), which

spanned roughly 24,000–19,000 cal yr BP (e.g., Allen and Holdaway, 2009). However, the alternating sands and clays of the Lake Mungo lunette that formed during the LGM suggest that lake levels varied between wet periods following floods and periods of drying that exposed at least part of the lake floor (Bowler et al., 2012; Fitzsimmons et al., 2014; Stern, 2015). Likewise, the abundance of stone tools, hearth sites, and other archaeological materials found in the LGM-aged dunes indicate at least periodic human presence (Stern et al., 2013; Fitzsimmons et al., 2014; Stern, 2015). The question is whether human occupation on the lakeshore coincided with periods of low lake level, wetter phases, or both? Was the lake stable or periodically drying out completely and then refilled by floodwater, and how do these changes track with an Aboriginal presence on the lakeshore? Interactions between climate change, lake hydrology, and Aboriginal peoples remain difficult to disentangle from current evidence. The issue is complicated by the mismatch between the millennial time spans represented by the sedimentary hydrological record and the subdecadal evidence represented by each archaeological site, some of which are the remains of a single

meal. MAP is continuing to conduct rigorous and systematic recording, dating, and assessing of archaeological remains and their associated sediments in partnership with the three traditional tribal groups of the Willandra Lakes region: Paakantyi/Barkandji, Ngiyampaa, and Mutthi Mutthi. As part of MAP, otoliths recovered from Aboriginal hearth sites offer an opportunity to examine water conditions at Lake Mungo during the LGM in greater detail and on timescales commensurate with human lives.

In a previous study (Long et al., 2014), oxygen isotopes and trace elements were analysed across the age increments of fish otoliths recovered from a series of Aboriginal hearth sites at Lake Mungo dating to the LGM (19,490–19,330 and 19,420–19,220 cal yr BP at 95.4% probability). The hearth otoliths all showed an increasing trend in both Sr/Ca ratios and oxygen isotopes (Fig. 2). Increases in Sr/Ca ratios are typically linked with fish movements to regions of high salinity (Zimmerman, 2005; Kerr et al., 2007; Macdonald and Crook, 2010). Moreover, preferential  $^{16}\text{O}$  removal during evaporation causes water  $\delta^{18}\text{O}$  to increase (Washburn and Urey, 1932; Craig et al., 1963), which would be recorded in the fish otoliths. The results, therefore, seemed to support the “easy prey” hypothesis proposed by Bowler (1998), whereby the fish entered into Lake Mungo with, or after, a flood and subsequently became trapped by evaporative conditions that cut off the lake from the rest of the Willandra system. It was then hypothesized that the trapped fish were targeted by human occupants, who took advantage of an assumed high-salinity-induced supine state of the fish, to “scoop [them] up in shallow waters” (Bowler, 1998, p. 148). Other LGM records also suggest that it was a cooler, drier, and dustier period in Australia (McTainsh and Lynch, 1996; Hesse et al., 2004; Barrows et al., 2007; Reeves et al., 2013). In combination, these factors and the otolith records were interpreted as evidence for strong evaporation, increasing salinity, and a drop in water levels at Lake Mungo (Long et al., 2014). However, this interpretation did not take into account mass balance effects, which could shed light on the relative roles of water inflow and evaporation

on changes in the isotopic composition of the water and hence the otoliths.

Isotopic mass balance models provide a theoretical framework to simulate and quantitatively interpret isotopic signals in lakes (Gibson et al., 2016). Under constant forcing, a closed lake will eventually reach a steady state in its mass balance if the volumes of water lost via evaporation and inflowing water are equal. Yet, volumetric mass balance does not equate to isotopic mass balance because this also depends on the mean isotope ( $\delta$ ) values of evaporating and inflowing water fluxes ( $F_E$  and  $F_{in}$ , respectively), following the generalised form  $\delta_L = (V_L\delta_L + F_{in}\delta_p + F_E\delta_E) / (V_L + F_{in} + F_E)$ , where  $\delta_E$  is a function of  $\delta_L$  via isotopic fractionation (e.g., Dinçer, 1968; Gonfiantini, 1986; Gibson et al., 1996; Gibson and Edwards, 2002; Jones et al., 2005; Rohling, 2016; Lacey and Jones, 2018). These studies used models that combine mass balance and isotopic mass balance to quantitatively assess the relative influence of different parameters on the isotopic composition of the water and can provide updated interpretations of archaeological and sediment records. For example, coupled isotope and mass balance models for Lake Ohrid, one of the oldest and deepest lakes in Europe, suggest that precipitation was up to 26% higher during the early Holocene than in the present day and 44% lower during the LGM (Lacey and Jones, 2018). The application of such models was also able to show that even though rainfall was much lower during the LGM, it was still high enough over the lake to support arboreal vegetation and provide a refugium for people during this time (Lacey and Jones, 2018).

In another example, this time focused on drought interpretations from sediment records, Rohling (2016) used mass balance models to test the assumption that if a lake isotope record suggested regional drying, it indicated a period of poor crop yields for nearby farmers. The study demonstrated that crop-growing potential could actually be improving while the lake records (usually inferred from oxygen isotope ratios) suggest that water levels were dropping. This study highlights the need to consider the different hydrological fluxes, catchments, and surface areas relevant to lakes vs. fields when inferring drought events from sedimentary lake records. Quantitative modelling of lake systems is an essential tool for revealing setting-specific relationships and controls on water  $\delta^{18}\text{O}$  and improving archaeological and environmental interpretations (Jones, 2013; Gibson and Reid, 2014; Jones et al., 2016; Rohling, 2016).

To date, no mass balance modelling of the relationship between  $\delta^{18}\text{O}$  and changes in palaeolake systems has been conducted for the Willandra Lakes region. Unlike the lakes of the modelling studies cited above (Jones et al., 2005; Rohling, 2016; Lacey and Jones, 2018), Lake Mungo contains no modern water to measure fluxes and properties or hydrological patterns to observe. Given that such currently dry lakes lack surface water, quantitative modelling in palaeolake systems relies on certain assumptions. While observations from nearby river systems can be used to approximate source-water  $\delta^{18}\text{O}$  for the model, humidity over the lake surface and hence the precise  $\delta^{18}\text{O}$  of evaporated vapour is unknown.

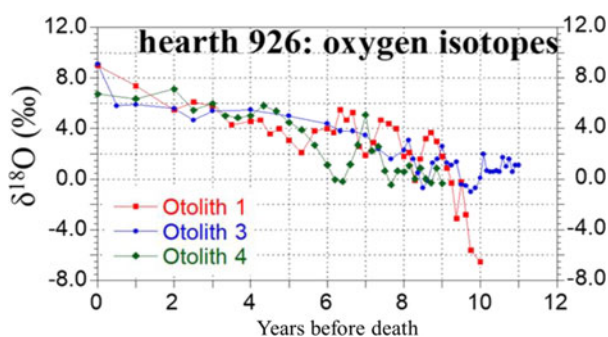


**Figure 2.** (color online) The oxygen isotope values plotted against otolith age lines as years before death for each of the otoliths collected from hearth 926 (adapted from Long et al., 2014). Adult life is on the left side of the x-axis and juvenile stage is on the right side of the x-axis.

Despite these limitations, simple models can be used to test proposed past hydrological scenarios for physical consistency and to estimate at least the sign and order of magnitude of past changes, using sensitivity tests to determine the dependence of the reconstructions on initial assumptions. The present study uses this approach for Lake Mungo to reveal the major controls on otolith  $\delta^{18}\text{O}$  in a quantitatively consistent manner.

In this study, we revisit the otolith oxygen isotope results from the Lake Mungo hearths (Long et al., 2014). We develop a box model for lake filling and drying based on the dimensions of the Willandra Lakes, modern evaporation rates for the region, and mass balance principles, including the Craig-Gordon model for oxygen isotope fractionation during evaporation (Craig and Gordon, 1965). This model is used to investigate how the oxygen isotopes of Lake Mungo would have changed, given Bowler's (1998) "easy prey" hypothesis. In this hypothesis, the Willandra Lakes were episodically filled by flood events followed by evaporation-driven isolation of Lake Mungo from the other lakes in the system, which eventually culminated in the desiccation of Lake Mungo.

## METHODS

### Site description

Lake Mungo is one of 13 major (currently dry) palaeolakes that make up the Willandra Lakes system. These lakes existed intermittently in cycles of wet and dry conditions throughout the Quaternary until they dried out completely at  $\sim 14.5$  ka (Bowler, 1998; Bowler et al., 2012; Fitzsimmons et al., 2014). This series of basins is situated in arid New South Wales, Australia. Based on data from Pooncarie (Mulurulu station), 46 km north of Mungo, the average annual rainfall is 281 mm, with the lowest annual total at 58 mm and the highest at 803 mm, based on 135 years of data from 1882 to 2017 (Australian Government Bureau of Meteorology, 2020a). The mean annual evaporation rate for the region is 2000 mm/yr, based on at least 10 years of records from 1975 to 2005, and seasonal evaporation rates range from 200 mm in the Southern Hemisphere winter (June, July, August) to 900 mm in the Southern Hemisphere summer (December, January, February) (Australian Government Bureau of Meteorology, 2020b). The region was inscribed on the UNESCO World Heritage list in 1981 as a site of national and international significance for its testament to both the cultural history of the Aboriginal people and the record of climatic and environmental changes throughout the Quaternary (Bowler et al., 1970; Bowler, 1998; Fitzsimmons et al., 2014; Stern, 2015).

A key feature of the Willandra Lakes region is the sand/clay dunes (lunettes), which have built up on the windward side of each basin. Based on the topography of the lake system and the sedimentary characteristics of the lunettes, it is inferred that these lakes were once connected, forming an overflow outlet for the Lachlan River (Bowler et al., 1970, 1976).

They were filled by large pulses of water that flowed from the Southern Tablelands of the Great Dividing Range down the Lachlan River into the Willandra Creek (Bowler et al., 1976; Bowler, 1998; Kemp and Rhodes, 2010). This water sequentially filled Lake Mulurulu and then Lakes Garnpung and Leaghur (Fig. 1). Lake Leaghur appears to have had two outflow points. The first is an overflow into Lake Mungo, the terminal lake in the system, via a shallow sill that separates the two lake basins. The second outflow is via the Willandra Creek, which then continues past Lake Mungo to feed into the outer Arumpo and Chibnalwood Lakes before eventually reaching the Prungle and Benenong Lakes farther to the south (Magee, 1991; Barrows et al., 2020; Jankowski et al., 2020).

### Study species

The main fish species found in hearth sites at Lake Mungo is the golden perch (*Macquaria ambigua* [Richardson] 1845). The golden perch is a long-lived species, which is today found throughout the Murray-Darling Basin, including the Lachlan River, preferring these predominately lowland, warmer, turbid, slow-flowing rivers (Lintermans, 2007). These fish can tolerate a wide range of salinities (0–33 ppt) and temperatures (4–37°C), and both juveniles and subadults can even survive in seawater (Langdon, 1987). In modern systems, golden perch do not naturally congregate near the shoreline of lakes. Instead, they inhabit deep pools ( $\sim 3$ –8 m) with woody debris, undercut banks, or rocky ledges (Cadwallader, 1979; Cadwallader and Backhouse, 1983; Battaglione and Prokop, 1987) and are usually fished using rods from small boats. Juvenile fish feed on aquatic insect larvae and microcrustaceans, while adults eat mainly shrimp, yabbies, small fish, and benthic aquatic insect larvae (Lintermans, 2007). Successful spawning and recruitment of golden perch typically require elevated water temperatures and flooding (Humphries et al., 1999; Mallen-Cooper and Stuart, 2003; Ye et al., 2008; King et al., 2009). The otoliths of golden perch, like those of many other species, grow continuously and deposit annual marks (light and dark bands) that represent fast and slow growth zones tracking seasonal environmental changes. These, when viewed in thin section, have been validated for ageing fish up to 22 years, according to release-recapture fish studies (Anderson et al., 1992; Stuart, 2006).

### Constructing the steady-state model

#### Data sources

This study focuses on comparing model results with oxygen isotope measurements from three otoliths collected from a single hearth (926) by MAP in 2009. The fish otolith oxygen isotope analysis was previously conducted and published as part of Long et al. (2014). The otoliths of hearth 926 recorded a  $\delta^{18}\text{O}$  increase of 7‰ over 6 years (otolith 926-4), 9‰ over 8.5 years (otolith 926-3), and 15‰ over 10 years (otolith 926-1) (Fig. 2).



A simple steady-state model was constructed to examine the influence of the hydraulic controls on lake water  $\delta^{18}\text{O}$  in the main Willandra Lakes system, with an emphasis on Lake Mungo. The hydrological setting of Lake Mungo, and the lake system more broadly, affects water  $\delta^{18}\text{O}$ , which in turn is recorded in the  $\delta^{18}\text{O}$  of the preserved otoliths. The isotopic starting point for the model is based on river records from the nearby Barwon-Darling River system (Hughes et al., 2012).

### *Establishing lake volumes and surface areas*

To construct the model, maximum water level, surface area, and volume were calculated for each lake. Initially, the maximum water level in each of the four modelled lake basins was established using a digital elevation model (DEM) from the scanning radar topography mission, provided by Geoscience Australia. Here, the maximum water level was controlled by the height of the outlet channel connecting each basin to the next in the chain (Bowler et al., 2012). Using DEM, the maximum lake level was defined as the highest closed 1-m contour line that resulted in separate lake basins. Next, surface areas and volumes were determined by excluding all contours that fell outside the highest closed 1-m contour line in each lake. The surface area was then calculated as the number of pixels in this contour, where each pixel represents a known unit area. To determine lake volume, the surface area was calculated by identifying pixels in 10-cm-depth intervals from the base of the lake to the highest closed 1-m contour line and integrating the series to estimate the volume at each respective 10-cm height.

### *Establishing mass balance conditions for the model*

The starting point for the model is that all lakes are full; effectively, this hypothetically represents the aftermath of a large flood event, per the Bowler (1998) hypothesis. The conditions required to maintain maximum lake levels are defined by water fluxes, specifically: (1) the rate of evaporation from each lake's surface, (2) the extra water that is needed to push water from one lake to the next, and (3) the amount of water needed to maintain the height of the next lake in the sequence. For example, for the water height of Lake Mungo to be maintained in a steady state, it needs to receive as much water from Lake Leaghur as it is losing via evaporation. For Lake Leaghur to remain full, it needs to receive as much water as it loses through evaporation as well as loss to Lake Mungo, where the latter is equivalent to the amount Lake Mungo loses via evaporation. Thus, the basic relationship between water fluxes representing the inflow, evaporation, and outflow required to maintain lakes in mass balance is given by:

$$F_w = F_E + F_{out} \quad (1)$$

where  $F_w$  is the water flux entering the lakes,  $F_E$  is the flux of water lost to evaporation, and  $F_{out}$  is the water flux needed to

maintain the heights of the lakes lower in the sequence. When  $F_w = F_E + F_{out}$ , the lake level is stable because loss via evaporation is compensated exactly by inflowing water. When  $F_w < F_E$ , the lake level will fall until empty because evaporation dominates. When  $F_w > F_E$ , inflowing water dominates over evaporation, so the lake level will rise until full and then overflow (i.e.,  $F_{out}$  becomes  $>0$ ). Similar expressions of these water fluxes for a chain or string of lakes are considered in Gibson and Reid (2014) and Gat and Bowser (1991).

The volume of water lost to evaporation from the first lake in the system is given by its surface area multiplied by the evaporation rate. The amount of outflow required is the surface area multiplied by the evaporation rate for each lake farther down the system (see Fig. 3).

The water flux entering the Willandra Lakes system that is required to keep the water levels at a constant height can be expressed as:

$$F_w = SA_1E + SA_2E + SA_3E + SA_4E \quad (2)$$

where  $F_w$  is water flux entering the system,  $SA_1$ ,  $SA_2$ ,  $SA_3$ , and  $SA_4$  are the surface areas of the lakes from top to bottom of the Willandra sequence, and  $E$  is the evaporation rate for the region. If no water flows out of Lake Mungo, then to maintain stable lake levels throughout the model system, the outflow for the top lake in the sequence must be equal to the sum of the surface area multiplied by the evaporation rate for each lake farther down in the sequence, or:

$$F_{out} = SA_2E + SA_3E + SA_4E \quad (3)$$

This gives us the amount of water needed to maintain all the lakes at mass balance after an initial filling event. Now that we have set up the model for maintaining water mass balance, we turn to establishing the isotopic equilibrium conditions.

### *Establishing isotopic equilibrium in the model*

Several variables affect the  $\delta^{18}\text{O}$  of water bodies. In the model presented here, we take into account the following: surface area and volume of the lakes; the regional evaporation rates (annual, winter, and summer); equilibrium and kinetic effects on the fractionation of water oxygen isotopes during evaporation; and the connections between the lakes. Given the shallowness of the lakes (maximum depth is  $\sim 7$ – $8$  m), their large surface area to volume ratios (Lake Mungo was  $\sim 140$  km<sup>2</sup> when full; Barrows et al., 2020), and the high wind speeds in the region (Mildura airport's mean monthly wind speed is between 9 and 20 km/hr (Australian Government Bureau of Meteorology, 2020c), the lakes are assumed to be well mixed. No direct lake-water oxygen isotope measurements are available because the modern lake system is dry and has not seen substantial water levels for the past  $\sim 16,000$  yr (Fitzsimmons et al., 2014). Therefore, the isotopic starting point for the model is estimated based on  $\delta^{18}\text{O}$  records from the nearby Barwon-Darling River as outlined in detail below

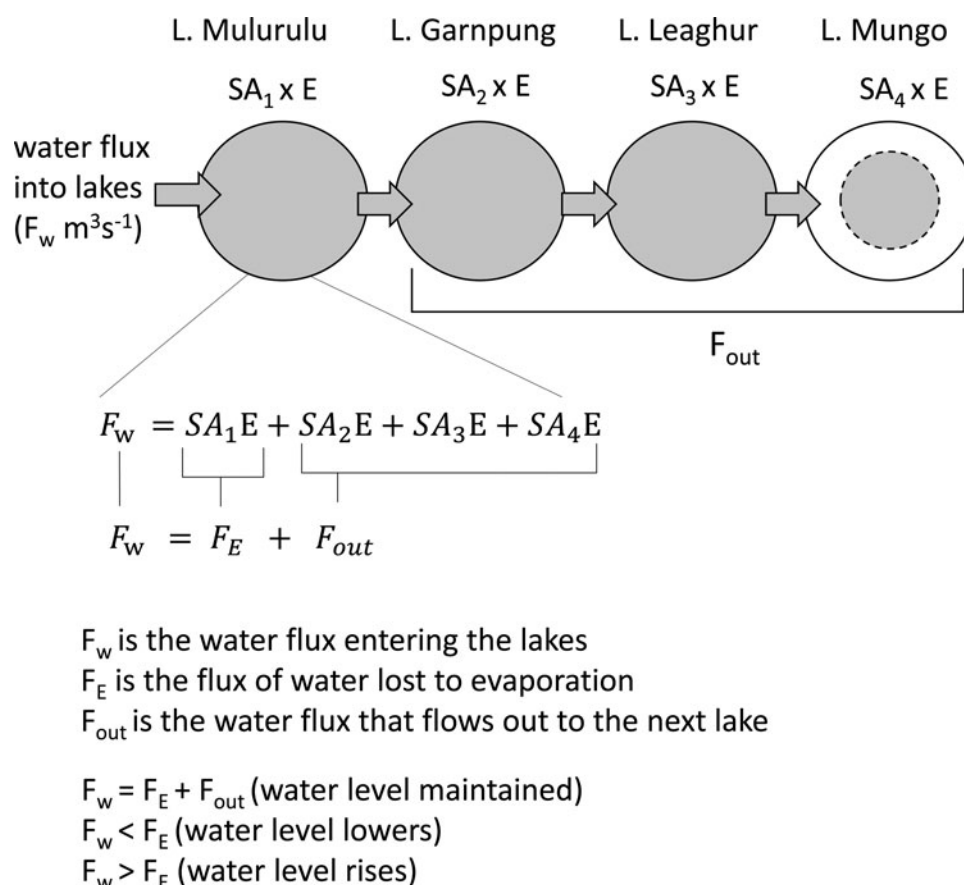


**Figure 3.** Schematic representation of the water flux entering the Willandra Lakes system as expressed by equations 1, 2, and 3. Note the equation shown is for the specific case of Lake Mulurulu and in the model is adjusted appropriately for each lake downstream.

(Hughes et al., 2012). The following variables are not considered in the model as there are no robust data available for this site at ~20 ka: humidity, temperature, groundwater input/output, and salinity.

It should be noted that although the water  $\delta^{18}\text{O}$  value used as a starting point for the model influences the final equilibrium  $\delta^{18}\text{O}$  value, it does not influence the rate or degree of change over time, which is what we are interested in for this study. We thus chose to use a water  $\delta^{18}\text{O}$  starting point of -8‰, based on studies of water  $\delta^{18}\text{O}$  in the nearby Barwon-Darling River (Meredith et al., 2009; Hughes et al., 2012). During high-flow events, like those that once filled the Willandra Lakes, ephemeral tributaries of the Barwon-Darling River contribute  $^{18}\text{O}$ -depleted water to the system. For example, Hughes et al. (2012) found that Darling River water at Bourke during the January 2004 high-flow event had a  $\delta^{18}\text{O}$  of -8.32‰ relative to -3.23‰ in water measured upstream at Brewarrina. Fluvial input near Bourke of  $^{18}\text{O}$ -depleted water from the Culgoa River, a normally dry tributary, caused the ~5‰ decrease in water  $\delta^{18}\text{O}$  (Hughes et al., 2012). We assume for the Willandra Lakes model that a large-scale flood event filled the lakes over a period of days, resulting from an intense rainfall event(s). The isotopic composition of the source water in such a scenario is

likely to be lighter (depleted in  $^{18}\text{O}$ ) than the composition of mean rainfall for the local or source region.

Using a -8‰ starting water  $\delta^{18}\text{O}$  value, the equation for the isotopic steady state is given by:

$$F_{in} \Delta t \delta_P = F_E \Delta t (\delta_L - x) + F_{out} \Delta t \delta_L \quad (4)$$

where  $\delta_p$  is the isotopic composition of precipitation or water entering the lakes,  $\delta_L$  is the isotopic composition of the lake water, and  $\delta_L - x$  gives the fractionation-related reduction in  $\delta^{18}\text{O}$  relative to the source liquid. At a typical ambient temperature of 15–20°C, equilibrium fractionation results in approximately  $x = 10$  (Gonfiantini, 1986; Froehlich et al., 2005; Rohling, 2016). In natural arid environments, this liquid-vapour offset can range from ~6‰ to 13‰, as measured respectively in evaporating water pans in arid Australia (Skrzypek et al., 2015; Gonfiantini et al., 2018) and the ephemeral Lake Gara Niba in the Algerian Sahara, northern Africa (Gonfiantini et al., 2018).  $\Delta t$  is the time step used in the model to calculate how the system evolves through time. In the model, evaporation causes the surface layer of each lake to become enriched with  $^{18}\text{O}$ , and the isotopically heavier surface water is then instantaneously mixed through the rest of the water column before being passed on to the

next lake in the sequence. Correspondingly, the first lake in the sequence was replenished with  $-8‰$  water.

### Running the steady-state model: scenarios

The first phase of the steady-state model involved setting up a series of connected boxes with the same dimensions as the Willandra Lakes basins and filling these instantly with water of  $\delta^{18}\text{O}$  equal to  $-8‰$ , simulating a massive flood event into the dry basins. The lake water was then maintained at mass balance (inflow = outflow + evaporation), while the water  $\delta^{18}\text{O}$  was allowed to adjust with evaporation and inflow according to equation 4. This was maintained for 20 years. We then used the  $\delta^{18}\text{O}$  value of water in Lake Mungo at the end of 20 years as the starting point for the second phase of the model, whereby we cut off inflow to Lake Mungo and allowed the water to evaporate.

We tested five different versions of the steady-state model, and the parameters of these are summarised in Table 1. In scenarios A, B, and C, we set  $F_E$  to the annual average evaporation rate for the region, which is 2000 mm/yr (Australian Government Bureau of Meteorology, 2020b); in scenarios B and C, we changed the degree of evaporative fractionation in equation 4 from  $x = 10$  (equilibrium) to  $x = 6$  and  $x = 14$ , respectively, as a sensitivity test for changes in fractionation due to kinetic effects in natural arid environments (Skrzypek et al., 2015; Gonfiantini et al., 2018). In scenarios D and E, we changed  $F_E$  from the modern annual average evaporation rate for the region (2000 mm/yr) to the winter (800 mm/yr) and then summer (3600 mm/yr) evaporation rates, respectively (Australian Government Bureau of Meteorology, 2020b). This provides sensitivity tests with respect to the model's response to different evaporation rates.

**Table 1.** Summary of the modelled scenarios for the Willandra Lakes; evaporation rates are based on historical records for the region from the Australian Government Bureau of Meteorology (2020b), and starting water values are estimated based on studies of nearby river systems (Hughes et al., 2012).

Scenario	Parameters
A	Starting water value = $-8‰$ , Evaporation rate = 2000 mm/yr, $x$ in equation 4 = 10 (equilibrium conditions)
B	Starting water value = $-8‰$ , Evaporation rate = 2000 mm/yr, $x$ in equation 4 = 6 (kinetic effects)
C	Starting water value = $-8‰$ , Evaporation rate = 2000 mm/yr, $x$ in equation 4 = 14 (kinetic effects)
D	Starting water value = $-8‰$ , Evaporation rate = 800 mm/yr (winter evaporation), $x$ in equation 4 = 10 (equilibrium conditions)
E	Starting water value = $-8‰$ , Evaporation rate: 3600 mm/yr (summer evaporation), $x$ in equation 4 = 10 (equilibrium conditions)

## RESULTS

### Lake volume and surface area

The surface area and volume of Lake Mungo are shown as functions of water level in Figure 4. We found negligible changes in the volume between 1 and 2 m water depths and a near-linear increase in volume from 2 to 7.5 m water depth, to a maximum volume of  $\sim 5.5 \times 10^8 \text{ m}^3$ . The surface area shows no appreciable increase until  $\sim 1.5 \text{ m}$  water depth, where it increases rapidly to  $\sim 1 \times 10^8 \text{ m}^2$  at 4 m water depth and then remains relatively stable until the maximum depth is achieved.

### Mass balance modelling

The results of the mass balance portion of the model, to the left of the dashed vertical line in Figure 5, show that the modelled water  $\delta^{18}\text{O}$  of each lake basin increases as a function of both time and distance down the system. At Mulurulu, the first lake in the sequence, the modelled  $\delta^{18}\text{O}$  of the lake water remains close to the  $-8‰$  of the inflow in all four scenarios, only increasing by 1–2‰ over 20 years. In contrast, the modelled water  $\delta^{18}\text{O}$  values at Lake Mungo, the terminal lake in the sequence, increase rapidly before beginning to plateau.

#### Scenario A: evaporation set to 2000 mm/yr, equilibrium scenario, $x = 10$

In scenario A,  $F_E = 2000 \text{ mm/yr}$  and  $x = 10$ , the modelled  $\delta^{18}\text{O}$  of water in Lake Mungo increases by  $\sim 18‰$  in five years and eventually levels off at  $\sim 10$  years, at a value of 14‰ (a total change of 22‰), which is maintained until the first part of the model ends at 20 years (Fig. 5A). The end value of 14‰ is used as the start of the second part of the model when inflow to Lake Mungo is ceased, and the water is left to evaporate until the lake is essentially dry (10 cm deep). Following the cessation of inflow, the modelled water  $\delta^{18}\text{O}$  for Lake Mungo increases by 16‰ in two years and continues to increase rapidly to beyond the limits of the graph.

#### Scenario B: evaporation set to 2000 mm/yr, $x = 6$

In scenario B, also with  $F_E = 2000 \text{ mm/yr}$ , we use  $x = 6$  to allow for evaporation under reduced fractionation compared to equilibrium, which results in a lesser increase in the modelled Lake Mungo water  $\delta^{18}\text{O}$ , namely 11‰ in five years and flattening at  $\sim 15$  years to a value of 5.5‰ (a total change of 13.5‰); this is maintained until the first part of the model ends at 20 years (Fig. 5B). In the second part of the model, when inflow to Lake Mungo ceases, the modelled water  $\delta^{18}\text{O}$  increases by 10.5‰ in two years and continues to increase rapidly to beyond the limits of the graph.

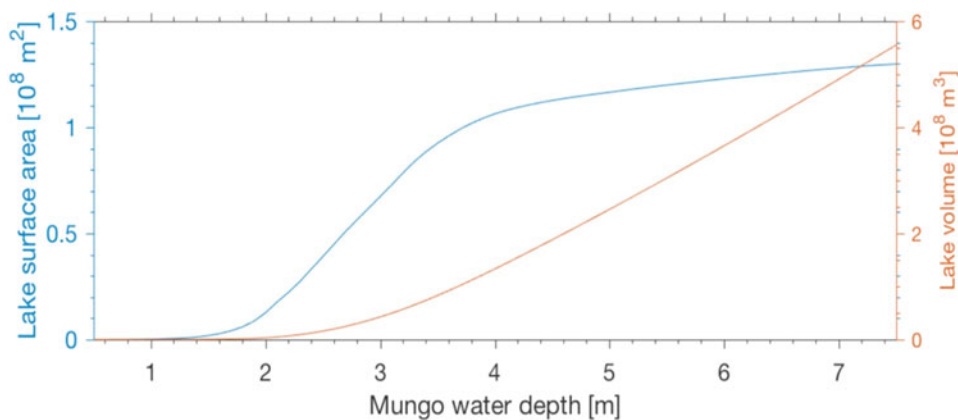


**Figure 4.** (color online) Modelled change in Lake Mungo’s surface area and volume with depth.

*Scenario C: evaporation set to 2000 mm/yr,  $x = 14$*

In scenario C, also with  $F_E = 2000$  mm/yr, we use  $x = 14$  to allow for substantial kinetic fractionation effects, which results in a greater increase in the modelled Lake Mungo water  $\delta^{18}\text{O}$ , namely 25‰ in five years and flattening within 12 years to a value of 23‰ (a total change of 31‰); this is maintained until the first part of the model ends at 20 years (Fig. 5C). In the second part of the model, when inflow to Lake Mungo ceases, the modelled water  $\delta^{18}\text{O}$  increases by 11‰ in two years and continues to increase rapidly to beyond the limits of the graph.

*Scenario D: evaporation set to 800 mm/yr, equilibrium scenario,  $x = 10$*

Assuming that the modern winter evaporation rate applies year-round, a sensitivity test with a low annual evaporation-rate (scenario D) causes the lake water  $\delta^{18}\text{O}$  to increase more slowly toward isotopic equilibrium. At Lake Mungo, the water  $\delta^{18}\text{O}$  increases by ~9‰ in the first five years of mass balance conditions, reaching ~13‰ at 20 years (a total change of 21‰). In the second phase, when inflow into Lake Mungo is cut off, the modelled water  $\delta^{18}\text{O}$  values

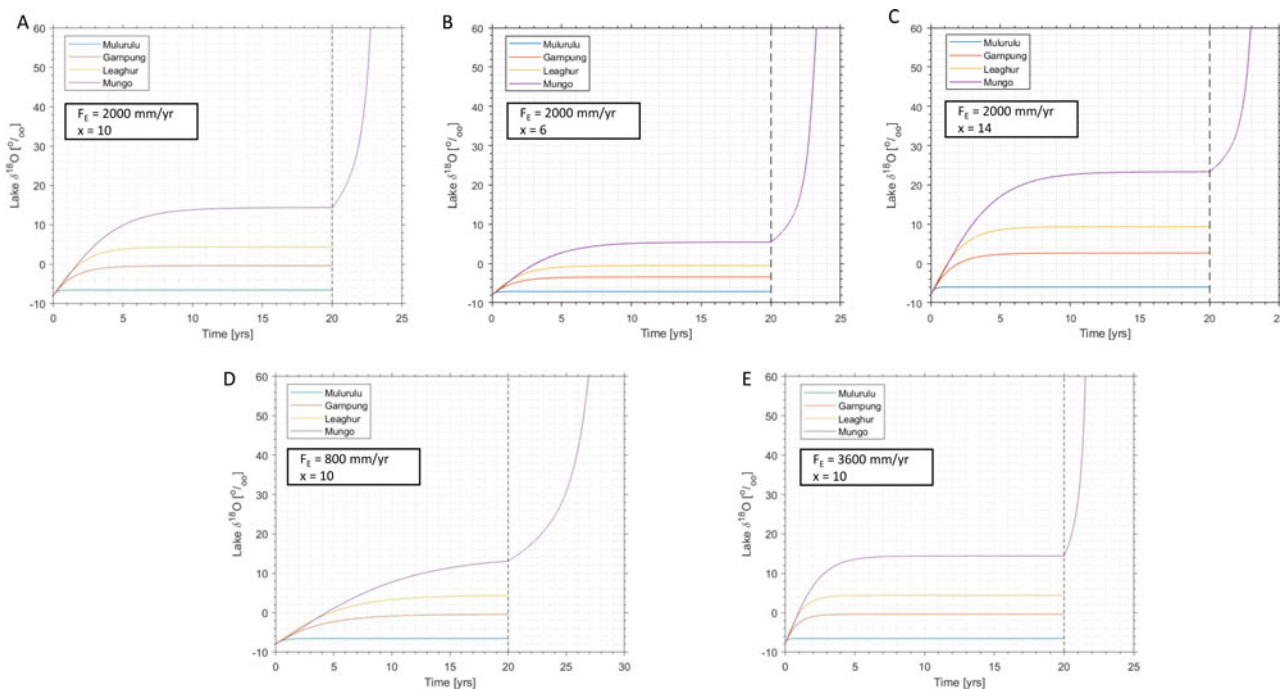


**Figure 5.** (color online) Modelled output for changes in the water  $\delta^{18}\text{O}$  of the Willandra Lakes system when the lake levels are maintained in mass balance for 20 years (to the left of the dashed vertical line) and the changes in the water  $\delta^{18}\text{O}$  of Lake Mungo when it is cut off from the other lakes and left to evaporate to dryness (10 cm deep) after those 20 years (to the right of the dashed vertical line). Five different scenarios are shown: (A) evaporation rate is set to 2000 mm/yr,  $x$  is set to 10 in equation 4; (B) evaporation rate is set to 2000 mm/yr,  $x$  is set to 6 in equation 4; (C) evaporation rate is set to 2000 mm/yr,  $x$  is set to 14 in equation 4; (D) evaporation rate is set to 800 mm/yr,  $x$  is set to 10 in equation 4; (E) evaporation rate is set to 3600 mm/yr,  $x$  is set to 10 in equation 4.



increase by 5‰ in the first year and 18‰ over five years (Fig. 5D).

*Scenario E: evaporation set to 3600 mm/yr, equilibrium scenario,  $x = 10$*

Assuming that the modern summer evaporation rate applies year-round, a sensitivity test with a high annual evaporation rate (scenario E) results in a faster increase in water  $\delta^{18}\text{O}$  during phase 1, with Lake Mungo water  $\delta^{18}\text{O}$  increasing by 22‰ in the first five years, culminating in a  $\delta^{18}\text{O}$  of  $\sim 14\%$  after 20 years (Fig. 5E). In the second phase, when inflow is cut off to Lake Mungo, the modelled water  $\delta^{18}\text{O}$  values increase sharply by 14‰ in the first year and by  $>60\%$  over two years.

## DISCUSSION

Under water mass balance conditions (inflow = evaporation + outflow), the water  $\delta^{18}\text{O}$ s will eventually approach isotopic equilibrium, a point at which there is no measurable change in the isotopic composition of the water; we refer to this point as “isotopic balance.”

In the results for the mass balance portion of the model, to the left of the dashed vertical line in Figure 5, the  $\delta^{18}\text{O}$ s of the different lakes progress similarly to different points of isotopic balance. The modelled water  $\delta^{18}\text{O}$  for Lake Mulurulu at the top of the sequence remains fairly low and close to the  $-8\%$  of incoming water in all scenarios. The lakes farther down the sequence (Leaghur, Garpung, and Mungo) reach successively higher isotopic balance points than does Lake Mulurulu. These results are a direct consequence of evaporation and the connections between the lakes, with each lake passing on isotopically heavier water (i.e., higher  $\delta^{18}\text{O}$ ) than the water it received from the upstream lake. Ultimately, this causes lakes farther from the primary water source to reach higher  $\delta^{18}\text{O}$  levels than those closer to the source. These results further demonstrate the string-of-lakes effect on water  $\delta^{18}\text{O}$ , as discussed by Gat and Bowser (1991) and Gibson and Reid (2014). If we had modelled water mass balance for Lake Mungo in isolation, the dependence of Lake Mungo water  $\delta^{18}\text{O}$  on processes in the lakes higher in the system would have been neglected.

### Comparison between the models and the otoliths

The impact of removing inflow on the  $\delta^{18}\text{O}$  of Lake Mungo water is shown to the right of the dashed vertical line in Figure 5. This is the point at which we isolated Lake Mungo and allowed the water to evaporate at the given rate until the lake was effectively dry (10 cm deep). Any fish that were living in the lake during the full extent of this trend would have died and been deposited on the lake floor. The fish otoliths that are the focus of this and the previous study (Long et al., 2014) were collected from hearth sites on the lakeshore, which suggests that they did not die naturally in the lake but were collected and eaten. The original interpretation of the increasing trends in the hearth otolith  $\delta^{18}\text{O}$  records proposed that they resulted

from water changes associated with progressive drying out and lowering of lake levels (Long et al., 2014). In all scenarios tested here, the change in water  $\delta^{18}\text{O}$  values when Lake Mungo is cut off and evaporating is much more rapid and of much greater amplitude than the changes recorded in the hearth otoliths. Within five years of inflow cut-off, the  $\delta^{18}\text{O}$  in all scenarios increases by  $>18\%$ . In scenario E, this even happens in two years (Fig. 5E). When we compare this to the maximum change recorded in the hearth otolith  $\delta^{18}\text{O}$  records—15‰ increase over 10 years (otolith 926-1; Fig. 2)—it becomes apparent that it is improbable that these fish were collected from a lake evaporating to dryness.

The results of this study show that under mass balance conditions, represented to the left of the dashed line in Figure 5, the modelled water  $\delta^{18}\text{O}$  of Lake Mungo increases to a point and then flattens. This happens in all five scenarios. These trends closely follow those observed in the hearth otoliths, in particular otolith 926-1, which shows a sharper increase in early life and a flatter trend in later life (Fig. 2). The total increase in hearth otolith  $\delta^{18}\text{O}$  is in the order of 10–15‰ over 10 years (otolith 926-1). This rate of change is most similar to the results for winter evaporation rate scenario D, where the increase in modelled water  $\delta^{18}\text{O}$  for Lake Mungo under mass balance conditions is 16‰ in 10 years (Fig. 5D).

Although the increasing trend in the hearth otoliths from Lake Mungo was initially interpreted (Long et al., 2014) in a qualitative manner in terms of inflow cut-off and subsequent lake desiccation, supporting the easy prey hypothesis (Bowler, 1998), our model-based quantitative assessment indicates that this can no longer be supported. Instead, we find that hearth otolith  $\delta^{18}\text{O}$  records are more representative of a recently flooded lake that is maintained in mass balance under relatively low evaporation conditions ( $<800$  mm/yr). That is, the otolith records are registering a change in oxygen isotopes with evaporation but not a change in lake volume and thus level.

Given the similarities between the winter mass balance model results (scenario D) and the otolith observations, we infer that the golden perch living in Lake Mungo between  $\sim 19$  and 19.5 ka were living in a mass-balanced system with a steady lake level, which gradually developed toward isotopic mass balance (equilibrium). We contend that it is highly unlikely that Lake Mungo evaporated to dryness during the period represented by the fishbone hearths. The rapid trend in water  $\delta^{18}\text{O}$  that would characterise evaporating lake conditions is not reflected in the hearth otolith data. This reinterpretation of the otolith records fits well with recent work at Lake Mungo, which suggests increased availability of surface water during the LGM as a result of lower evaporation rates and increased runoff (Barrows et al., 2020).

### Fish otolith $\delta^{18}\text{O}$ and lake level modelling compared to sedimentary records

Sedimentary archives provide a broad range of information concerning lake hydrology, and optically stimulated

luminescence dating has proven invaluable for putting this information into a chronological sequence (Fitzsimmons et al., 2014; Barrows et al., 2020; Jankowski et al., 2020). The difficulty comes with matching these records with an Aboriginal presence on the lakeshore. Otoliths and shells from hearth sites and middens are already being used to radiocarbon date hearth sites on the lakeshore and link them to the sediments in which they lie (Stern, 2015), but there is further value in these otoliths and shells. The subannual records in otoliths can add detail to the local lake level history, experienced by people in the past. When coupled with mass balance modelling, as shown here, we can start to rule out some scenarios for lake conditions and add weight to others.

### Otolith: diagenetic, cooking, and trash disposal effects

Modern golden perch fish otoliths are typically composed entirely of aragonite. Diagenetic effects like heating can cause the aragonite to recrystallise into the more stable polymorph calcite. In archaeological otolith samples, the absence of calcite is usually a good indication that an otolith has not been affected by chemical alteration. Two of the ancient hearth otoliths were tested using X-ray diffraction, and neither were found to contain measurable calcite (Long et al., 2014). This provides some assurance that recrystallisation has not occurred.

Regarding the effect of cooking on fish otolith oxygen isotopes, Disspain et al. (2016) applied a range of different cooking methods to black bream and found that otoliths that had been heated had lower mean  $\delta^{18}\text{O}$  compared to the control group. Differences in  $\delta^{18}\text{O}$  between heat-treated otoliths and the control group ranged from -1.09 to -1.47‰, except for the otoliths that were burnt. Burnt otoliths were visibly blackened with a chalky texture, and these had  $\delta^{18}\text{O}$  values 4.37‰ lower than the control. This is similar to the results of cooking experiments conducted by Andrus and Crowe (2002), who found that the  $\delta^{18}\text{O}$  of burnt Atlantic croaker (*Micropogonius undulatus*) and catfish (*Bagre marinus*) otoliths were 1.8–3.1‰ lower than the control sample. The study by Long et al. (2014) avoided any otoliths that showed signs of burning (blackened surface), but they may have experienced heating. If we take into account the possibility that heating affected hearth otolith  $\delta^{18}\text{O}$  values, they should all be 1–2‰ higher, as heating would have caused the original  $\delta^{18}\text{O}$  value to decrease. There would be no change in the slope of the observed trend, and so this does not increase support for an evaporating lake scenario.

### Evaporation rate, equilibrium, and kinetic fractionation

The annual average evaporation rate during the LGM is unknown. Likewise, the effect of ambient conditions on the isotopic fractionation of water during evaporation is unknown for the LGM. Therefore, we tested multiple evaporation rates

and both equilibrium and kinetic values for  $x$  in equation 4 to determine the effect these have on the modelled water  $\delta^{18}\text{O}$ . The results show that the evaporation rate affects the speed at which the water  $\delta^{18}\text{O}$  increases toward isotopic balance, while the fractionation rate controls the height of that balance point. All the scenarios with the same  $x$  value in equation 4 will eventually reach the same isotopic balance point, but the time this takes differs. In the summer scenario (Fig. 5E), which had the highest evaporation rate, the increase in modelled water  $\delta^{18}\text{O}$  for Lake Mungo occurs quite quickly, reaching isotopic balance in 10 years. In contrast, the winter evaporation scenario (Fig. 5D), with the lowest evaporation rate, yields a modelled water  $\delta^{18}\text{O}$  curve for Lake Mungo that is flatter and only reaches 13‰ in the 20 years of the model. If we extended the time frame for this portion of the model, it would eventually flatten out at ~14‰. By changing the value for  $x$  from 10 in scenario A to 14 in scenario C (Fig. 5C), we increase the isotopic balance point from ~14 to ~23‰. By reducing the value for  $x$  to 6 in scenario B (Fig. 5B), we reduce the isotopic balance point to ~5.5‰. Even with this reduced value of  $x$ , the change in the water  $\delta^{18}\text{O}$  of Lake Mungo, 11‰ in 5 years, is still greater and faster than the change observed in the otoliths (15‰ in 10 years). Regardless of there being only equilibrium ( $x = 10$ ) or equilibrium + kinetic ( $x = 10 \pm 4$ ), based on water bodies evaporating in similarly arid environments (Gonfiantini et al., 2018) and fractionation during evaporation, the change in water  $\delta^{18}\text{O}$  when Lake Mungo is cut off and left to evaporate is still much more pronounced than that seen in the otoliths. For the model presented here, the only way that the trend can be flattened to more closely match the otoliths is by changing the evaporation rate.

### Model limitations

All models have limitations around what can and cannot be inferred (Box, 1976). The model created here is not a true-to-life simulation of climate and lake conditions in the Willandra Lakes region during the LGM. Instead, it is a simplified model that only considers the amount of water needed to fill the lakes, the annual evaporation rate, and basic isotopic theory for fractionation of water during evaporation. There are usually subannual to decadal changes in temperature, humidity, water input, evaporation rate, and other factors that are simply unknown for this period at the scale needed to compare to the life of a fish.

The mass balance models presented here do not include contributions from groundwater. It has been suggested by Bowler et al. (2012) that during the final drying of the lower lakes in the system, an influx of seasonal high-salinity groundwater would have produced clay dunes with a high gypsum content. So far, the only lake where high gypsum clays are observed on the lunettes is at Chibnalwood/Arumpo, which is below Lake Leaghur in the sequence and not directly connected to Lake Mungo. These lakes are not considered in the present scenario, and there is no evidence of a gypsum clay phase at Lake Mungo (Bowler et al., 2012).

In the nearby Darling River, groundwater exchanges were found to increase the river water Cl<sup>-</sup> content (increasing the salinity), but the depletion in the stable isotope values by mixing with depleted groundwater was found to be overwhelmed by evaporative enrichment (Meredith et al., 2009). Those authors could only identify the impact of groundwater input on the oxygen isotopes by sampling at a high spatial and temporal resolution a short distance of the river. Similar conclusions were reached by Simpson and Herczeg (1991), who observed that groundwater influx had a major impact on salinity levels when Darling River waters were low, whereas the impact on the isotopes of the river water was minor. In the present study, we are comparing our model outputs to the otolith records, which at best contain an annual average trend and are unlikely to pick up the short-term influence of groundwater isotopic input. We have therefore decided not to include this in our model.

The salinity of the water in the Willandra Lakes in the past is unknown, but it is expected that any salts accumulating in the upstream lakes would be flushed downstream during flood events (Bowler et al., 2012). This would result in increased salinity during evaporation and higher salinity at lakes lower in the chain. In marine or near-marine salinities, evaporation can result in a reversal in the enrichment process of the oxygen isotopes during evaporation (Gonfiantini, 1986; Gat, 1995). There is no reversing trend evident in the otolith oxygen isotope values, and so it is unlikely that salinity was high enough to cause this effect; thus, it is not considered in the model scenarios.

If humidity were included in the model, we would likely find a change in the evaporative slope. Heavy isotope enrichment is considerable when humidity is low, but the effect is reduced when humidity is higher (Gat and Bowser, 1991). Humidity also has a role to play in limiting the isotopic enrichment of the lake water. At humidity 0.75 (75%), the limiting value for a lake of 0‰ is +8‰. At humidity 0.50 (50%), the same lake has a limiting value of ~24‰, and at humidity 0.25 (25%), the limit is >40‰. Again, there are no records for humidity at Lake Mungo during the LGM, but a follow-up mass balance model could test different scenarios to see what effect this has on the oxygen isotope trends.

## CONCLUSIONS

Our reappraisal of the  $\delta^{18}\text{O}$  records preserved in golden perch (*Macquaria ambigua*) otoliths from archaeological contexts at the Lake Mungo UNESCO World Heritage Site indicates that the fish did not die in a lake that was cut off from the river system and evaporating to dryness. Our calculations instead suggest that the annual evaporation rate for the region was lower than it is today and that lake levels were more or less stable (i.e., the fish were living in a mass-balanced system, and the otolith  $\delta^{18}\text{O}$  increase resulted from the gradual development of the ambient water toward isotopic balance). The trend in otolith  $\delta^{18}\text{O}$  values was most similar to those of the water when the lakes were full and evaporative rates were set to 800 mm/yr. Our results also have implications

for the interpretation of Aboriginal fishing practices. The hypothesis that people were taking advantage of sluggish oxygen-starved golden perch in a drying-out lake system does not seem to be supported. Hence, consideration needs to be given to other fishing techniques and thus the role of fish in the diet. Development of the implications will require more oxygen isotope records across otolith (or shell) age increments from the Willandra Lakes region and further refinement of the modelling to account for variation in environmental factors such as humidity, temperature, precipitation, and groundwater processes.

## ACKNOWLEDGMENTS

We would like to thank the Traditional Tribal Groups of the Willandra Lakes Region and thank the support of the Willandra Lakes Region Aboriginal Advisory Group and guidance set out in their Research Code of Practice. We would like to thank Nicola Stern and Nathan Jankowski for providing comments on the sections related to the archaeology and geology of Lake Mungo and the Willandra Lakes, and Matthew Jones for providing comments on the modelling aspects of this study. Thanks also to the reviewers and QR Editors who provided insightful comments that greatly improved the final manuscript. This research was supported in part by ARC DP150100487 and ARC DP1092966. Long was supported in part by a postdoctoral fellowship with the ARC Centre of Excellence in Australian Biodiversity and Heritage. The model code can be found at <https://github.com/dave-heslop74/Mungo-model>.

## REFERENCES

- Allen, H., Holdaway, S., 2009. The archaeology of Mungo and the Willandra Lakes: looking back, looking forward. *Archaeology in Oceania* 44, 96–106.
- Anderson, J.R., Morison, A.K., Ray, D.J., 1992. Validation of the use of thin-sectioned otoliths for determining the age and growth of golden perch, *Macquaria ambigua* (Perciformes: Percichthyidae), in the lower Murray-Darling Basin, Australia. *Australian Journal of Marine and Freshwater Resources* 43, 1103–1128.
- Andrus, C.F.T., Crowe, D.E., 2002. Alteration of otolith aragonite: effects of prehistoric cooking methods on otolith chemistry. *Journal of Archaeological Science* 29, 291–299.
- Andrus, C.F.T., Crowe, D.E., Sandweiss, D.H., Reitz, E.J., Romanek, C.S., 2002. Otolith delta 18O record of mid-Holocene sea surface temperatures in Peru. *Science* 295, 1508–1511.
- Australian Government Bureau of Meteorology, 2020a. Monthly Rainfall Data: Pooncarie (Murluru Station) (accessed July 16, 2020). [http://www.bom.gov.au/jsp/ncc/cdio/weatherData/av?p\\_nccObsCode=139&p\\_display\\_type=dataFile&p\\_startYear=&p\\_c=&p\\_stn\\_num=047024](http://www.bom.gov.au/jsp/ncc/cdio/weatherData/av?p_nccObsCode=139&p_display_type=dataFile&p_startYear=&p_c=&p_stn_num=047024).
- Australian Government Bureau of Meteorology, 2020b. Average Annual, Monthly and Seasonal Evaporation (accessed November 7, 2020). [http://www.bom.gov.au/jsp/ncc/climate\\_averages/evaporation/index.jsp](http://www.bom.gov.au/jsp/ncc/climate_averages/evaporation/index.jsp).
- Australian Government Bureau of Meteorology, 2020c. Monthly Climate Statistics: Mildura Airport (accessed July 22, 2020). [http://www.bom.gov.au/climate/averages/tables/cw\\_076031.shtml](http://www.bom.gov.au/climate/averages/tables/cw_076031.shtml).
- Barrows, T.T., Fitzsimmons, K.E., Mills, S.C., Tumney, J., Pappin, D., Stern, N., 2020. Late Pleistocene lake level history of Lake Mungo, Australia. *Quaternary Science Reviews* 238, 106338.



- Barrows, T.T., Juggins, S., De Deckker, P., Calvo, E., Pelejero, C., 2007. Long-term sea surface temperature and climate change in the Australian-New Zealand region. *Paleoceanography* 22, PA2215.
- Battaglione, S., Prokop, F., 1987. Golden Perch, *AGFACTS* A3.2.2. N.S.W Department of Agriculture, Sydney, Australia.
- Bowler, J.M., 1998. Willandra Lakes revisited: environmental framework for human occupation. *Archaeology in Oceania* 33, 120–155.
- Bowler, J.M., Gillespie, R., Johnston, H., Boljkovac, K., Boljkovac, K., 2012. Wind v water: glacial maximum records from the Willandra Lakes. In: Haberle, S.G., David, B. (Eds.), *Peopled Landscapes: Archaeological and Biogeographic Approaches to Landscapes*. Terra Australis Series 34. ANU Press, Canberra, pp. 271–296.
- Bowler, J.M., Hope, G.S., Jennings, J.N., Singh, G., Walker, D., 1976. Late Quaternary climates of Australia and New Guinea. *Quaternary Research* 6, 359–394.
- Bowler, J.M., Johnston, H., Olley, J.M., Prescott, J.R., Roberts, R.G., Shawcross, W., Spooner, N.A., 2003. New ages for human occupation and climatic change at Lake Mungo, Australia. *Nature* 421, 837–840.
- Bowler, J.M., Jones, R., Allen, H., Thorne, A.G., 1970. Pleistocene human remains from Australia: a living site and human cremation from Lake Mungo, western New South Wales. *World Archaeology* 2, 39–60.
- Box, G.E.P., 1976. Science and statistics. *Journal of the American Statistical Association* 71, 791–799.
- Cadwallader, P.L., 1979. Distribution of native and introduced fish in the Seven Creeks River system, Victoria. *Australian Journal of Ecology* 4, 361–385.
- Cadwallader, P.L., Backhouse, G.N., 1983. *A Guide to the Freshwater Fish of Victoria*, Melbourne, Victoria: Victorian Government Printing Office, on behalf of the Fisheries and Wildlife Division, Ministry for Conservation, 1–249.
- Campana, S.E., 1999. Chemistry and composition of fish otoliths: pathways, mechanisms and applications. *Marine Ecology Progress Series* 188, 263–297.
- Craig, H., Gordon, L., 1965. Deuterium and oxygen-18 variations in the ocean and the marine atmosphere. In: Tongiorgi, E. (Ed.), *Stable Isotopes in Oceanographic Studies and Paleotemperatures*. Laboratorio di Geologia Nucleare, Pisa, Italy.
- Craig, H., Gordon, L.I., Horibe, Y., 1963. Isotopic exchange effects in the evaporation of water: 1, low-temperature experimental results. *Journal of Geophysical Research* 68, 5079–5087.
- Dinçer, T., 1968. The use of oxygen 18 and deuterium concentrations in the water balance of lakes. *Water Resources Research* 4, 1289–1306.
- Disspain, M.C.F., Ulm, S., Izzo, C., Gillanders, B.M., 2016. Do fish remains provide reliable palaeoenvironmental records? An examination of the effects of cooking on the morphology and chemistry of fish otoliths, vertebrae and scales. *Journal of Archaeological Science* 74, 45–59.
- Dufour, E., Van Neer, W., Vermeersch, P.M., Patterson, W.P., 2018. Hydroclimatic conditions and fishing practices at Late Paleolithic Makhadma 4 (Egypt) inferred from stable isotope analysis of otoliths. *Quaternary International* 471, 190–202.
- Fitzsimmons, K., Stern, N., Murray-Wallace, C.V., 2014. Depositional history and archaeology of the central Lake Mungo lunette, Willandra Lakes, southeast Australia. *Journal of Archaeological Science* 41, 349–364.
- Froehlich, K.F.O., Gonfiantini, R., Rozanski, K., 2005. Isotopes in lake studies: a historical perspective. In: Aggarwal, P.K., Gat, J.R., Froehlich, K.F.O. (Eds.), *Isotopes in the Water Cycle: Past, Present and Future of a Developing Science*. Springer-Verlag, Berlin, pp. 139–150.
- Gat, J.R., 1995. Stable isotopes of fresh and saline lakes. *Physics and Chemistry of Lakes* 60, 139–163.
- Gat, J.R., Bowser, C., 1991. The heavy isotope enrichment of water in coupled evaporative systems. In: Taylor, P., O'Neill, J.P., Kaplan, I.R. (Eds.), *Stable Isotope Geochemistry: A Tribute to Samuel Epstein Special Pu*. Geochemical Society, Washington, D.C., pp. 159–168.
- Geffen, A.J., Høie, H., Folkvord, A., Hufthammer, A.K., Andersson, C., Ninnemann, U., Pedersen, R.B., Nedreaas, K., 2011. High-latitude climate variability and its effect on fisheries resources as revealed by fossil cod otoliths. *ICES Journal of Marine Science* 68, 1081–1089.
- Gibson, J.J., Birks, S.J., Yi, Y., 2016. Stable isotope mass balance of lakes: a contemporary perspective. *Quaternary Science Reviews* 131, 316–328.
- Gibson, J.J., Edwards, T.W.D., 2002. Regional water balance trends and evaporation-transpiration partitioning from a stable isotope survey of lakes in northern Canada. *Global Biogeochemical Cycles* 16, 1026.
- Gibson, J.J., Edwards, T.W.D., Prowse, T.D., 1996. Development and validation of an isotopic method for estimating lake evaporation. *Hydrological Processes* 10, 1369–1382.
- Gibson, J.J., Reid, R., 2014. Water balance along a chain of tundra lakes: a 20-year isotopic perspective. *Journal of Hydrology* 519, 2148–2164.
- Gonfiantini, R., 1986. Environmental isotopes in lake studies. In: Fritz, P., Fontes, J.C. (Eds.), *Handbook of Environmental Isotope Geochemistry*. Vol. 2, *The Terrestrial Environment*, B. Elsevier, Amsterdam, The Netherlands, pp. 113–168.
- Gonfiantini, R., Wassenaar, L.I., Araguas-Araguas, L., Aggarwal, P.K., 2018. A unified Craig-Gordon isotope model of stable hydrogen and oxygen isotope fractionation during fresh or saltwater evaporation. *Geochimica et Cosmochimica Acta* 235, 224–236.
- Hesse, P.P., Magee, J.W., van der Kaars, S., 2004. Late Quaternary climates of the Australian arid zone: a review. *Quaternary International* 118–119, 87–102.
- Hughes, C.E., Stone, D.J.M., Gibson, J.J., Meredith, K.T., Sadek, M.A., Cendon, D.I., Hankin, S.I., Hollins, S.E., Morrison, T.N., 2012. Stable water isotope investigation of the Barwon-Darling River system, Australia. In: *Monitoring Isotopes in Rivers: Creation of the Global Network of Isotopes in Rivers (GNIR). Results of a Coordinated Research Project 2002–2006*. International Atomic Energy Agency, Vienna, pp. 97–110.
- Humphries, P., King, A., Koehn, J., 1999. Fish, flows and flood plains: links between freshwater fishes and their environment in the Murray-Darling River system, Australia. *Environmental Biology of Fishes* 56, 129–151.
- Jankowski, N.R., Stern, N., Lachlan, T.J., Jacobs, Z., 2020. A high-resolution late Quaternary depositional history and chronology for the southern portion of the Lake Mungo lunette, semi-arid Australia. *Quaternary Science Reviews* 233, 106224.
- Jones, M.D., 2013. What do we mean by wet? Geoarchaeology and the reconstruction of water availability. *Quaternary International* 308–309, 76–79.
- Jones, M.D., Cuthbert, M.O., Leng, M.J., McGowan, S., Mariethoz, G., Arrowsmith, C., Sloane, H.J., Humphrey, K.K., Cross, I.,



2016. Comparisons of observed and modelled lake  $\delta^{18}\text{O}$  variability. *Quaternary Science Reviews* 131, 329–340.
- Jones, M.D., Leng, M.J., Roberts, C.N., Türkeş, M., Moyeed, R., 2005. A coupled calibration and modelling approach to the understanding of dry-land lake oxygen isotope records. *Journal of Paleolimnology* 34, 391–411.
- Kalish, J.M., 1991. Oxygen and carbon stable isotopes in the otoliths of wild and laboratory-reared Australian salmon (*Arripis trutta*). *Marine Biology* 47, 37–47.
- Kemp, J., Rhodes, E.J., 2010. Episodic fluvial activity of inland rivers in southeastern Australia: palaeochannel systems and terraces of the Lachlan River. *Quaternary Science Reviews* 29, 732–752.
- Kerr, L., Secor, D., Kraus, R., 2007. Stable isotope ( $\delta^{13}\text{C}$  and  $\delta^{18}\text{O}$ ) and Sr/Ca composition of otoliths as proxies for environmental salinity experienced by an estuarine fish. *Marine Ecology Progress Series* 349, 245–253.
- King, A.J., Tonkin, Z., Mahoney, J., 2009. Environmental flow enhances native fish spawning and recruitment in the Murray River, Australia. *River Research and Applications* 25, 1205–1218.
- Lacey, J.H., Jones, M.D., 2018. Quantitative reconstruction of early Holocene and last glacial climate on the Balkan peninsula using coupled hydrological and isotope mass balance modelling. *Quaternary Science Reviews* 202, 109–121.
- Langdon, J.S., 1987. Active osmoregulation in the Australian bass, *Macquaria novemaculeata* (Steindachner), and the golden perch, *Macquaria ambigua* (Richardson) (Percichthyidae). *Marine and Freshwater Research* 38, 771–776.
- Leng, M.J., Lewis, J.P., 2014. Oxygen isotopes in molluscan shell: applications in environmental archaeology. *Environmental Archaeology* 21, 295–306.
- Leng, M.J., Marshall, J.D., 2004. Palaeoclimate interpretation of stable isotope data from lake sediment archives. *Quaternary Science Reviews* 23, 811–831.
- Lintermans, M., 2007. *Fishes of the Murray-Darling Basin: An Introductory Guide*. Murray-Darling Basin Commission, Canberra, Australia.
- Long, K., Stern, N., Williams, I.S., Kinsley, L., Wood, R., Sporic, K., Smith, T., et al., 2014. Fish otolith geochemistry, environmental conditions and human occupation at Lake Mungo, Australia. *Quaternary Science Reviews* 88, 82–95.
- Long, K., Wood, R., Williams, I.S., Kalish, J., Shawcross, W., Stern, N., Grün, R., 2018. Fish otolith microchemistry: snapshots of lake conditions during early human occupation of Lake Mungo, Australia. *Quaternary International* 463, 29–43.
- Macdonald, J.I., Crook, D.A., 2010. Variability in Sr:Ca and Ba:Ca ratios in water and fish otoliths across an estuarine salinity gradient. *Marine Ecology Progress Series* 413, 147–161.
- Magee, J.W.W., 1991. Late Quaternary lacustrine, groundwater, aeolian and pedogenic gypsum in the Prungle Lakes, southeastern Australia. *Palaeogeography, Palaeoclimatology, Palaeoecology* 84, 3–42.
- Mallen-Cooper, M., Stuart, I.G., 2003. Age, growth and non-flood recruitment of two potamodromous fishes in a large semi-arid/temperate river system. *River Research and Applications* 19, 697–719.
- Mannino, M.A., Thomas, K.D., Leng, M.J., Sloane, H.J., 2008. Shell growth and oxygen isotopes in the topshell *Osilinus turbinatus*: resolving past inshore sea surface temperatures. *Geo-Marine Letters* 28, 309–325.
- McTainsh, G.H., Lynch, A.W., 1996. Quantitative estimates of the effect of climate change on dust storm activity in Australia during the last glacial maximum. *Geomorphology* 17, 263–271.
- Meredith, K.T., Hollins, S.E., Hughes, C.E., Cendón, D.I., Hankin, S., Stone, D.J.M., 2009. Temporal variation in stable isotopes ( $^{18}\text{O}$  and  $^2\text{H}$ ) and major ion concentrations within the Darling River between Bourke and Wilcannia due to variable flows, saline groundwater influx and evaporation. *Journal of Hydrology* 378, 313–324.
- Olley, J.M., Roberts, R.G., Yoshida, H., Bowler, J.M., 2006. Single-grain optical dating of grave-infill associated with human burials at Lake Mungo, Australia. *Quaternary Science Reviews* 25, 2469–2474.
- Reeves, J.M., Barrows, T.T., Cohen, T.J., Kiem, A.S., Bostock, H.C., Fitzsimmons, K.E., Jansen, J.D., et al., 2013. Climate variability over the last 35,000 years recorded in marine and terrestrial archives in the Australian region: an OZ-INTIMATE compilation. *Quaternary Science Reviews* 74, 21–34.
- Rohling, E.J., 2016. Of lakes and fields: a framework for reconciling palaeoclimatic drought inferences with archaeological impacts. *Journal of Archaeological Science* 73, 17–24.
- Simpson, H.J., Herczeg, A.L., 1991. Salinity and evaporation in the River Murray basin, Australia. *Journal of Hydrology* 124, 1–27.
- Skrzypek, G., Mydłowski, A., Dogramaci, S., Hedley, P., Gibson, J.J., Grierson, P.F., 2015. Estimation of evaporative loss based on the stable isotope composition of water using *Hydrocalculator*. *Journal of Hydrology* 523, 781–789.
- Stern, N., 2015. The archaeology of the Willandra: its empirical structure and narrative potential. In: McGrath, A., Jebb, M.A. (Eds.), *Long History, Deep Time: Deepening Histories of Place*. ANU Press, Canberra, pp. 221–240.
- Stern, N., Tumney, J., Kajewski, P., 2013. Strategies for investigating human responses to changes in landscape and climate at Lake Mungo in the Willandra Lakes, southeast Australia. In: Frankel, D., Webb, J., Lawrence, S. (Eds.), *Archaeology in Technology and Environment*. Routledge, London, pp. 31–50.
- Stuart, I.G., 2006. Validation of otoliths for determining age of golden perch, a long-lived freshwater fish of Australia. *North American Journal of Fisheries Management* 26, 52–55.
- Washburn, E.W., Urey, H.C., 1932. Concentration of the  $\text{H}^2$  isotope of hydrogen by the fractional electrolysis of water. *Proceedings of the National Academy of Sciences* 18, 496–498.
- Weidman, C.R., Millner, R., 2000. High-resolution stable isotope records from North Atlantic cod. *Fisheries Research* 46, 327–342.
- Ye, Q., Cheshire, K., Fler, D., Centre, S.A.A.S., 2008. *Recruitment of Golden Perch and Selected Large-Bodied Fish Species Following the Weir Pool Manipulation in the River Murray, South Australia*. SARDI Research Report 303. SARDI Aquatic Sciences, Adelaide.
- Zimmerman, C.E., 2005. Relationship of otolith strontium-to-calcium ratios and salinity: experimental validation for juvenile salmonids. *Canadian Journal of Fisheries and Aquatic Sciences* 62, 88–97.